Laboratori Nazionali di Frascati

LNF-70/41

G. Baldacchini and V. Montelatici: A CONTRIBUTION TO THE STUDY OF DYNAMIC POLARIZATION BY SOLID EFFECT

Estratto da : Nuovo Cimento 68B, 253 (1970)

G. BALDACCHINI, *et al.*
11 Agosto 1970
Il Nuovo Cimento
Serie X, Vol. 68 B, pag. 253-281

A Contribution to the Study of Dynamic Polarization by Solid Effect.

G. BALDACCHINI and V. MONTELATICI
Laboratori Nazionali di Frascati del CNEN - Frascati

(ricevuto il 19 Febbraio 1970)

Summary. — The theory of solid effect is developed from a thermodynamical and statistical approach by introducing a chemical potential for each group of the spins of the system according to their states. The entropy production rate is written as a function of chemical potentials and transition probabilities. The mechanisms of the relaxation processes are specialized, and the energy balance among Zeeman and phonon energies and the energy flux to the heat bath is considered. In this way two coupled equations are obtained for the polarizations of ions and protons, which are linearized by using deduced relations, at stationary state, among the chemical potentials and the ion and proton relaxation times ratio, in the limit case when the electronic Boltzmann factor is transferred to protons. The proton relaxation time and the dynamic polarization at 6370 G, in the helium-temperature range are measured in LaMN crystals doped with 1% and 3.5% of neodymium ions. The experimental relaxation times are in good agreement with the theoretical values. Discrepancies are found concerning the dependance of relaxation times on the concentration of impurities. The experimental dynamic polarization values, whose maximum is about 20% for 1% doping, show a marked effect of direct cooling by the electron system, an effect already reported at lower magnetic fields by other authors.

1. – Introduction.

In this article the behaviour of the dynamic polarization of protons in a crystalline diamagnetic substance, containing paramagnetic impurities, is considered.

A particular aspect of the dynamic polarization, the well-known « solid effect », is treated.

In such an effect two kinds of magnetic moments (paramagnetic ions and protons), which are assumed to have spin $\frac{1}{2}$, are coupled by a magnetic dipolar interaction; it is supposed they are acted on by a static magnetic field, H_0.

Such an interaction permits simultaneous transitions of two different kinds of spins to occur; one transition occurs at the frequency $\nu_{\pm} = \nu_S \pm \nu_I$, where ν_S is the ionic resonance frequency, the other one occurs at the frequency ν_I, where ν_I is the proton resonance frequency. When the power of an electromagnetic field at one of the side frequencies is sufficiently high, one observes an enhancement of the thermal equilibrium proton signal at the temperature T_0 of the heat bath.

The solid effect was observed the first time by ÜEBERSFELD in 1958 in liquids [1], subsequently it was extended to ionic solids [2] by JEFFRIES in 1960.

The most important properties of the effect were soon understood; later on LEIFSON and JEFFRIES [3], JEFFRIES and SCHMUGGE [4], ABRAGAM and BORGHINI [5] gave more accurate theories.

Some of these authors (L.J.S.) gave a theory based on the rate equations method of BLOEMBERGEN [6,7], other authors (A.B.) gave a theory which is an extension of the theories by REDFIELD [8] and PROVOTOROV [9]. The problem of the dynamic polarization, which involves high-intensity pumping power of the electromagnetic field, is correctly formulated through the density matrix formalism (A.B), in which a spin temperature is assigned to each Zeeman system and another one associated with each interaction.

The analytical solution of the so formulated problem is possible only in the so-called high-temperature approximation, because of the mathematical difficulties of the method (*). However the result, given by the most simplified theory (L.J.S.), is not different from that of the density matrix theory when the spectral lines are well resolved. This last case is the so-called « solid effect ».

In this article the solid effect is considered from a statistical and thermodynamical point of view [10].

---

[1] J. ÜBERSFELD, J. L. MOTCHANE and E. ERB: *Coll. Int. LXXXVI Sur la Résonance Magnétique 1958*, Edit. du Centre Nat. Rech. Scientifique.

[2] C. D. JEFFRIES: *Phys. Rev.*, **117**, 1056 (1960).

[3] C. D. JEFFRIES and O. S. LEIFSON: *Phys. Rev.*, **122**, 1781 (1961).

[4] T. J. SCHUMUGGE and C. D. JEFFRIES: *Phys. Rev.*, **138**, A 1785 (1965).

[5] M. BORGHINI and A. ABRAGAM: *Proc. in Low Temperature Physics*, vol. 4 (Amsterdam, 1964).

[6] N. BLOEMBERGEN, E. M. PURCELL and R. V. POUND: *Phys. Rev.*, **73**, 679 (1948).

[7] N. BLOEMBERGEN: Thesis, Leiden (1948).

[8] A. G. REDFIELD: *Phys. Rev.*, **98**, 1787 (1955).

[9] B. N. PROVOTOROV: *Sov. Phys. JETP*, **14**, 1126 (1962).

(*) Recently a transcendental solution has been obtained under particular conditions: M. A. KOZHUSHNER: *Sov. Phys. JETP*, **29**, 136 (1969).

[10] V. MONTELATICI: *Nuovo Cimento*, **32**, 1613 (1964).

The rate equations, which in the earlier theory are written *ad hoc* by introducing the right terms to take into account the simultaneous transitions (in analogy to the cross-relaxation terms of BLOEMBERGEN [11]), are obtained directly as a consequence of the initial formulation.

The system of ion and proton spins is considered as the set of all possible pairs formed by an ion and a proton spin. If n and N are the proton spin and the ion spin numbers in a cubic centimeter respectively, one can distribute the nN possible pairs among the $(2S+1)(2I+1)=4$ unperturbed energy levels, according to their energy.

By associating a chemical potential to each level, each system has a ratio of the mean occupation numbers regulated by the difference of its chemical potentials [12].

Then the internal entropy production is written as a function of the chemical potentials and of the time variations of the number of the pairs for each level. Under the ideal condition that the ion polarization is transferred to protons, a simple relation is obtained between chemical potentials and spin-lattice relaxation times at the stationary state.

Since in this ideal case the chemical potentials can easily be determined, the relaxation times can be determined as well.

In this way a criterion to linearize the differential equations, which gives the evolution of the polarizations of ions and protons, is obtained. The linearization is performed by using approximations, which improve as the relaxation times approach their limit values.

In the second part of the article an experimental apparatus is described and experimental results are presented. Their interpretation is discussed.

In the first Appendix a calculation of the transition probability involving the ion-proton spin interaction is developed. In the second Appendix some features of spin lattice relaxation times are discussed.

2. – Spin system statistics and thermodynamics.

N ion spins (S) and n proton spins (I) in the unit volume are considered with a weak magnetic dipolar interaction among them. All other types of interactions are disregarded. The spins are imbedded in a crystal lattice, whose thermal vibrations can be represented by the phonon system. Therefore we suppose an interaction between spins and phonons exists, which is able to

---

[11] N. BLOEMBERGEN, S. SHAPIRO, P. S. PERSHAN and J. O. ARTMAN: *Phys. Rev.*, **114**, 445 (1959).

[12] V. MONTELATICI: *Nuovo Cimento*, **47** B, 104 (1967).

induce time random transitions bringing each system to the Boltzmann thermal equilibrium ([13]) at the temperature T_0 of the heat bath.

When the whole system is acted on by a sufficiently high magnetic field H_0, the Zeeman energies are greater than the dipolar energy, so that the spin Hamiltonian, to a good approximation, is given by

$$(1) \qquad \mathscr{H}_z = + |\gamma_S| \hbar \bar{S} \cdot \bar{H}_0 - \gamma_I \hbar \bar{I} \cdot \bar{H}_0 ,$$

where $\bar{S}$ and $\bar{I}$ are the spin operators, $\gamma = g\beta h^{-1}$ is the gyromagnetic ratio for systems (S) and (I) respectively, with $\gamma_S < 0$ and $\gamma_I > 0$, g is the Landé factor, and β the Bohr magneton.

Under these conditions the $(2S+1)\cdot(2I+1)$ possible states of the ion-proton system are those shown in Fig. 1, in which the ions have an « effective spin » $S = \frac{1}{2}$ and the protons a spin $I = \frac{1}{2}$.

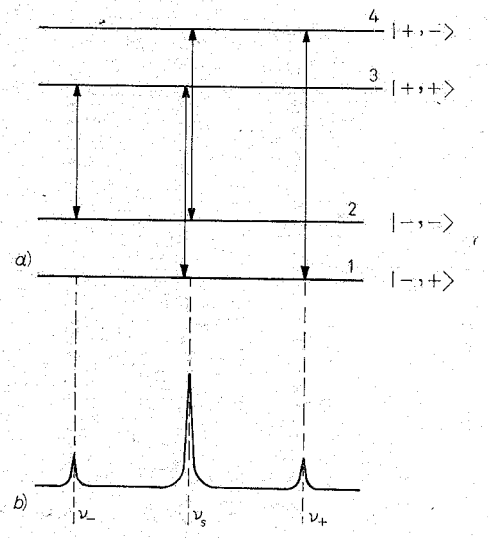

Fig. 1. – Schematic of the unperturbed energy levels *a*) and their state $|m_S, m_I\rangle$; an idealized ion paramagnetic absorption in a constant magnetic field *b*).

The presence of the weak dipolar interaction and the thermal vibrations allow for transitions occurring among an energy level and all the others, and are responsible for four relaxation mechanisms having the following selection rules ([14]):

a) $\Delta m_S = \pm 1, \ \Delta m_I = 0 ,$

b) $\Delta m_I = \pm 1, \ \Delta m_S = 0 ,$

c) $\Delta m_S = \Delta m_I = \pm 1 ,$

d) $\Delta m_S = -\Delta m_I = \pm 1 .$

Cases *c*) and *d*) are quasi-ionic transitions showing a simultaneous flip of the two kinds of spins; and cases *a*) and *b*) are ion and proton transitions respectively.

When the system is irradiated by an electromagnetic field at a frequency $\nu_\pm$, with the magnetic vector of the field normal to the static magnetic field H_0, transitions of type *c*) and *d*) are induced.

([13]) A. ABRAGAM: *Phys. Rev.*, **98**, 1729 (1955).

([14]) A. ABRAGAM: *The Principles of Nuclear Magnetism* (Oxford, 1961).

The ions and protons in the system are distributed in four groups of pairs, $n_i^* = N_i n_i$, according to the energy of each level. If $E_i = \hbar H_0(|\gamma_S| m_S - \gamma_I m_I)$, with $m_S = \pm \frac{1}{2}$; $m_I = \pm \frac{1}{2}$ and $i = 1, 2, 3, 4$, is the energy of the i-th level, the partition function is [15]

$$Z_i = \frac{1}{n_i^*!}\left[\exp\left[-\frac{E_i}{kT_0}\right]\right]^{n_i^*}, \tag{2}$$

where T_0 is the heat-bath temperature.

Then the quantity n_i^* is related to the energy and to the chemical potential, μ_i, by the statistical expression

$$\frac{\partial F_i}{\partial n_i^*} \equiv \mu_i = E_i + kT_0 \log n_i^*, \tag{3}$$

where $F_i = -KT_0 \log Z_i$ is the free energy of the i-th level. The Gibbs relation is applicable to the system [16]

$$T_0 \mathrm{d}S = \mathrm{d}U + \mathrm{d}W - \sum_{i=1}^{4} \mu_i \mathrm{d}n_i^*, \tag{4}$$

where $\mathrm{d}W$ is zero because the magnetic field is constant, and the summation gives the internal entropy production due to the transition from one level to another at temperature T_0.

In the stationary state one has

$$\left(\frac{\mathrm{d}S}{\mathrm{d}t}\right)_{\mathrm{int}} = -\frac{1}{T_0} \sum \mu_i \frac{\mathrm{d}n_i^*}{\mathrm{d}t} = 0. \tag{5}$$

Consider now the transitions of type a) as chemical reactions:

$$n_1^* \rightleftarrows n_3^*, \qquad n_2^* \rightleftarrows n_4^*; \tag{6}$$

these relationships are equivalent to taking account of the reaction $N_- \rightleftarrows N_+$ twice. They give rise to the internal entropy production [16]

$$\left(\frac{\mathrm{d}S}{\mathrm{d}t}\right)_{\mathrm{int}\,S} = \frac{1}{2T_0}\left[(\mu_3 - \mu_1)\frac{\mathrm{d}(n_1^* - n_3^*)}{\mathrm{d}t} + (\mu_4 - \mu_2)\frac{\mathrm{d}(n_2^* - n_4^*)}{\mathrm{d}t}\right] = -\frac{nN}{2T_0}(\mu_3 - \mu_1)\dot{P}, \tag{7}$$

---

[15] L. D. Landau and E. M. Lifshitz: *Statistical Physics* (London, 1958).

[16] I. Prigogine: *Thermodynamics of Irreversible Processes* (London, 1961).

where $NP = N_+ - N_-$, and the property of the chemical potentials of being not independent has been used, that is

$$\mu_4 - \mu_2 = \mu_3 - \mu_1 . \tag{8}$$

By analogy, if the transitions of type *b*) are considered, one obtains

$$\left(\frac{\mathrm{d}S}{\mathrm{d}t}\right)_{\mathrm{int}\ I} = \frac{nN}{2T_0}(\mu_2 - \mu_1)\dot{p} ,$$

where $np = n_+ + n_-$. Therefore the relation (5) takes the form

$$\left(\frac{\mathrm{d}S}{\mathrm{d}t}\right)_{\mathrm{int}} = \frac{nN}{2T_0}[-\dot{P}(\mu_3 - \mu_1) + \dot{p}(\mu_2 - \mu_1)] . \tag{9}$$

On the other hand, keeping in mind that the time variations of the n_i^* are both a function of the thermally induced transition probabilities $w_{ij} \neq w_{ji}$, and of the transitions $W_{ij} = W_{ji}$ induced by external radiation ([17]),

$$\frac{\mathrm{d}n_i^*}{\mathrm{d}t} = \sum_{j=1}^{4}(n_j^* w_{ji} - n_i^* w_{ij}) + \sum_j W_{ij}(n_j^* - n_i^*) . \tag{10}$$

We obtain, after rearrangement, the explicit form of (5)

$$\left(\frac{\mathrm{d}S}{\mathrm{d}t}\right)_{\mathrm{int}} = -\frac{1}{T_0}\sum_{i=1}^{4}\mu_i \frac{\mathrm{d}n_i^*}{\mathrm{d}t} = -\frac{1}{T_0}\{(\mu_1 - \mu_2)[N(n_- w_{21} - n_+ w_{12}) + \tag{11}$$

$$+ (N_+ n_- w_{41} - N_- n_+ w_{14}) - (N_+ n_+ w_{32} - N_- n_- w_{23}) + W_+(N_+ n_- - N_- n_+) -$$

$$- W_-(N_+ n_+ - N_- n_-)] + (\mu_1 - \mu_3)[n(N_+ w_{31} - N_- w_{13}) - (N_+ n_- w_{41} - N_- n_+ w_{14}) +$$

$$+ (N_+ n_+ w_{32} - N_- n_- w_{23}) + W_+(N_+ n_- - N_- n_+) + W_-(N_+ n_+ - N_- n_-)]\} ,$$

where we have used $w_{21} = w_{43}$, $w_{12} = w_{34}$; $w_{13} = w_{24}$, $w_{31} = w_{42}$ and the relation (8). We also recall that $W^+ \equiv W_{41} = W_{14}$ and $W_- \equiv W_{32} = W_{23}$ are the induced transition probabilities at frequency $\nu_+ = \nu_S + \nu_I$ and $\nu_- = \nu_S - \nu_I$.

3. – The solid effect.

The spin system (S) is in thermal contact with the heat bath through the lattice vibrations. The particular mechanisms of the relaxation processes are responsable for the energy transfer occurring among them. The energy exchange between phonons and heat bath is supposed to occur in a characteristic time τ.

([17]) A. J. F. SIEGERT: *Phys. Rev.*, **76**, 1708 (1949).

A system of harmonic oscillators (Debye model) ([18]) is supposed to represent the phonon system to which the energy is given from the system (S). Such a mechanism is described by a first-order process (direct process) ([19]) which is dominant at low temperatures. In such a relaxation process a phonon at frequency ν_S is created when a spin jump happens from a higher state to a lower one.

If the rate of energy flux from the spins (S) is greater than the energy flux from phonons to the heat bath, the temperature of the phonon system is raised to a value $T > T_0$ (phonon bottleneck) ([20-22]). Therefore the transition probabilities for the system (S) are

$$w_{13}\left[h\left(\frac{\nu_S}{T}\right)\right]^{-1} = w_{31}\left[h\left(\frac{\nu_S}{T}\right)+1\right]^{-1} \equiv \alpha w, \tag{12}$$

where

$$h\left(\frac{\nu}{T}\right) = \left[\exp\left[\frac{2\pi\hbar\nu}{kT}\right]-1\right]^{-1}$$

is the mean phonon excitation number ([15]) at temperature T and frequency ν.

The interaction, in ionic solids, of the protons (I) with the phonons is very weak and therefore negligible ([23]). The relaxation is due to the ions (S); however an extra relaxation (for example, due to impurity, rotational level, etc.) is supposed to exist which brings the populations to the right Boltzmann equilibrium at temperature T_0. That is

$$w_{12}\exp\left[\frac{2\pi\hbar\nu_I}{2kT_0}\right] = w_{21}\exp\left[-\frac{2\pi\hbar\nu_I}{2kT_0}\right] \equiv w_I. \tag{13}$$

The simultaneous relaxation of a spin (S) and a spin (I) occurs at a frequency $\nu_\pm = \nu_S \pm \nu_I$.

Therefore one has

$$\begin{cases} w_{14}\exp\left[\frac{2\pi\hbar\nu_I}{2kT_0}\right]\left[h\left(\frac{\nu_+}{T}\right)\right]^{-1} = w_{41}\exp\left[-\frac{2\pi\hbar\nu_I}{2kT_0}\right]\left[h\left(\frac{\nu_+}{T}\right)+1\right]^{-1} \equiv \beta' w, \\ w_{23}\exp\left[-\frac{2\pi\hbar\nu_I}{2kT_0}\right]\left[h\left(\frac{\nu_-}{T}\right)\right]^{-1} = w_{32}\exp\left[\frac{2\pi\hbar\nu_I}{2kT_0}\right]\left[h\left(\frac{\nu_-}{T}\right)+1\right]^{-1} \equiv \beta' w, \end{cases} \tag{14}$$

([18]) J. M. ZIMAN: *Electrons and Phonons* (London, 1963).

([19]) *Spin Lattice Relaxation in Ionic Solids*, A. A. MANENKOV and R. ORBACH, reprints (London, 1966).

([20]) A. M. STONEHAM: *Proc. Phys. Soc.*, **86**, 1163 (1965).

([21]) P. L. SCOTT and C. D. JEFFRIES: *Phys. Rev.*, **127**, 32 (1962).

([22]) M. W. P. STRANDBERG: *Phys. Rev.*, **110**, 65 (1958).

([23]) N. BLOEMBERGEN: *Physica*, **15**, 386 (1949).

where α in (12) and β' in (14) are quantities depending on the dipolar interaction between protons and ions (see Appendix A).

As a consequence of the approximations we shall do below, we introduce in (14) the Boltzmann factors in order to obtain the right relaxation to the heat-bath temperature for the system (*I*).

We suppose that the mean number of excitations, at the two side frequencies $\nu_{\pm}$, are equal, then

$$h\left(\frac{\nu_+}{T}\right) = h\left(\frac{\nu_-}{T}\right) \equiv h^{**}\left(\frac{\tilde{\nu}}{T}\right) \tag{15}$$

and for simplicity we write $h(\nu_s/T) = h^*(\nu_s/T)$.

Using the relations (12), (13), (14) and (15) we explicit the relation (11) in the form

$$\begin{aligned}\left(\frac{\mathrm{d}S}{\mathrm{d}t}\right)_{\mathrm{int}} &= -\frac{1}{T_0}\sum_1^4 \mu_i \frac{\mathrm{d}n_i^*}{\mathrm{d}t} = -\frac{Nn}{2T_0}(\mu_1-\mu_2)\cdot \\ &\cdot\{-(p-p_0)\cosh\delta[2w_I-\beta' w(P_{**}^{-1}-P(\tilde{\nu}))]+W_+(P-p)-W_-(P+p)\}- \\ &-\frac{Nn}{2T_0}(\mu_1-\mu_3)\{-\alpha w[PP_*^{-1}-1]-\cosh\delta(1-pp_0)\beta' w[PP_{**}^{-1}-1]+ \\ &+W_+(P-p)+W_-(P+p)\} \equiv \frac{Nn}{2T_0}(\mu_2-\mu_1)\{\varphi\}+\frac{Nn}{2T_0}(\mu_3-\mu_1)\{\Phi\}\,.\end{aligned} \tag{16}$$

This expression will be used by putting to a good approximation $\cosh\delta \simeq 1$ and $1-pp_0 \simeq 1$, in the usual range of frequencies and temperatures.

Here

$$\delta = \frac{2\pi\hbar\nu_I}{2kT_0} = 2.4\cdot 10^{-5}\frac{\nu_I}{T_0}\frac{\mathrm{MHz}}{^\circ\mathrm{K}}\,,$$

and

$$P_{**}^{-1} = 2h^{**}\left(\frac{\tilde{\nu}}{T}\right)+1\,, \qquad P_*^{-1} = 2h^*\left(\frac{\nu_s}{T}\right)+1\,.$$

By comparing (9) and (16), we obtain the coupled differential equations: $\dot{p}-\varphi=0$, $\dot{P}+\Phi=0$.

In order to eliminate P_* and P_{**} we consider the energy balance among Zeeman energy, phonon energy and energy relaxed to heat bath at the frequencies ν_s and $\tilde{\nu} \simeq \nu_s+\nu_I \simeq \nu_s-\nu_I$ [24]. We obtain

$$\begin{cases}\dfrac{\mathrm{d}}{\mathrm{d}t}\left[h^*\left(\dfrac{\nu_s}{T}\right)-h^*\left(\dfrac{\nu_s}{T_0}\right)\right]2\tau = -\sigma\alpha(PP_*^{-1}-1)-(P_0^{-1}-P_*^{-1})\,, \\ \dfrac{\mathrm{d}}{\mathrm{d}t}\left[h^{**}\left(\dfrac{\tilde{\nu}}{T}\right)-h^{**}\left(\dfrac{\tilde{\nu}}{T_0}\right)\right]2\tau = -\sigma\beta'(PP_{**}^{-1}-1)-(P_0^{-1}-P_*^{-1})\,,\end{cases} \tag{17}$$

---

[24] B. W. FAUGHNAN and M. W. P. STRANDBERG: *Journ. Phys. Chem. Solids*, **19**, 155 (1961).

where $-P_0/w = T_s$ is the direct relaxation time of ions, and $\sigma = \tau E_Z$ (Zeeman energy)$/T_s$ E_{Ph} (phonon energy), with

$$E_{Ph} = 2\pi\hbar\nu\varrho\Delta[h(\nu/T_0) + \tfrac{1}{2}] = 2\pi\hbar\nu\varrho\Delta(2P_0)^{-1} \quad \text{and} \quad E_Z = 2\pi\hbar\nu NP_0/2.$$

In this relation $\varrho\cdot\Delta$ is the number of oscillator modes in the band Δ with density ϱ, and we made the approximations $E_Z(\nu_S) \simeq E_Z(\tilde{\nu})$, $E_{Ph}(\nu_S) \simeq E_{Ph}(\tilde{\nu})$ (*).

From (16) and (17) we obtain the coupled equations at the stationary state:

$$(18)\qquad \begin{cases} (p-p_0)\left[2w_I + \beta' \dfrac{w}{P_0}\dfrac{1-P_0P+\beta'\sigma(1-P^2)}{1+\beta'\sigma P/P_0}\right] + \\ \qquad\qquad + W_+(p-P) + W_-(p+P) = 0\,, \\ (P-P_0)\left[\dfrac{w}{P_0}\left(\dfrac{\alpha}{1+\alpha\sigma P/P_0} + \dfrac{\beta'}{1+\beta'\sigma P/P_0}\right)\right] + \\ \qquad\qquad + W_+(P-p) + W_-(P+p) = 0\,, \end{cases}$$

where the expressions inside the brackets represent the inverse of time constants (see Appendix B).

A microscopic calculation for coefficients α and β' gives: $\beta' = (N/n)\beta$ for the system (I), while

$$\alpha = \left(1-\sum\varepsilon_j^2\right)^2/\left(1+\sum\varepsilon_j^2\right)^2, \qquad \beta' = \beta = 4\sum\varepsilon_j^2/\left(1+\sum\varepsilon_j^2\right)^2,$$

for the system (S), where the summation is over all the protons (I). By analogy, the induced transition probabilities are

$W_\pm(\nu_S \pm \nu_I) = (N/n)\beta W(\nu_S)$ for system (I),

and

$W_\pm(\nu_S + \nu_I) = \beta W(\nu_S)$ for system (S),

where $W(\nu_S)$ is the transition probability induced by an electromagnetic field at frequency ν_S, (see Appendix A).

A block model, that we have used in order to obtain eqs. (18), is sketched in Fig. 2.

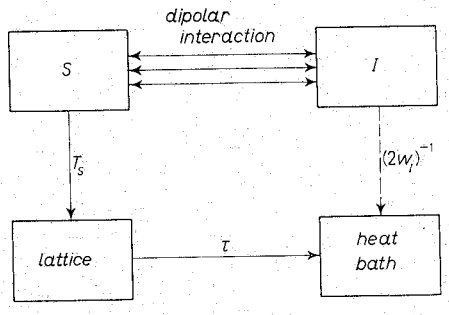

Fig. 2. – Block model of the spin-bath relaxation of the system S and I.

(*) One has initially three equations, which from these approximations reduce to two.

4. – Limit case, $p \to \pm P$.

The main aim, in the dynamic polarization, is to transfer the polarization of ion system (S) to proton system (I). The coupled equations (18) can be linearized in the variables p and P with certain approximations, which can be deduced in the limit case $p \to \pm P$, that is when the total transfer of polarization is performed from the system (S) to the system (I).

Under this condition we obtain, from relations (3), the expressions for the chemical potential differences of a function of Zeeman energies:

$$(\mu_3 - \mu_1) \pm (\mu_2 - \mu_1) = 2\pi\hbar(\nu_S \pm \nu_I) . \tag{19}$$

Therefore the population ratios are

$$\begin{cases} \dfrac{n_2^*}{n_1^*} = \dfrac{n_-}{n_+} = \exp\left[\dfrac{(\mu_2 - \mu_1) - 2\pi\hbar\nu_I}{kT_0}\right] = \\ \quad = \exp\left[\dfrac{\mp(\mu_3 - \mu_1) \pm 2\pi\hbar\nu_S}{kT_0}\right] \xrightarrow[\mu_3 - \mu_1 \to 0]{} \exp\left[\dfrac{\pm 2\pi\hbar\nu_S}{kT_0}\right] = \exp\left[\dfrac{\pm 2\pi\hbar\nu_I}{kT_*}\right], \\ \dfrac{n_3^*}{n_1^*} = \dfrac{N_+}{N_-} = \exp\left[\dfrac{(\mu_3 - \mu_1) - 2\pi\hbar\nu_S}{kT_0}\right] \xrightarrow[\mu_3 - \mu_1 \to 0]{} \exp\left[\dfrac{-2\pi\hbar\nu_S}{kT_0}\right]. \end{cases} \tag{20}$$

They show that the total transfer is possible only if

$$(\mu_3 - \mu_1) \to 0 , \qquad \mu_2 - \mu_1 = \pm 2\pi\hbar(\nu_S \pm \nu_I) . \tag{21}$$

$T_* = \pm T_0 \nu_I / \nu_S$ is the temperature taken by system (I) (*), whose resonance

(*) This result is also obtained in the theory which studies the behaviour of a spin system (S) in a rotating frame ([8,9,14]) at a temperature T_* different from T_0. For high intensity of the radiation field at frequency ν near ν_S, T_* follows the law

$$T_* = T_0 \frac{(\nu_S - \nu)^2 + \nu_L^2 + \gamma_S^2 H_1^2/(2\pi)^2}{\nu_S(\nu_S - \nu)} \simeq T_0 \frac{(\nu_S - \nu)^2 + \nu_L^2}{\nu_S(\nu_S - \nu)} ,$$

where H_1^2 is the squared radiation field and ν_L is a constant of the order of the line width. When $\nu = \nu_S \mp \nu_I$ and $\nu_L \ll \nu_I$, then $T_* = \pm T_0 \nu_I / \nu_S$. In the rotating frame the temperature T_* is also the temperature of system (I) which is put in thermal contact with system (S) by the action of the radiation field. Since the Hamiltonian of system (I), in the rotating frame, is the same as that in the laboratory frame, system (I) cools off or warms up at temperature T_*. This process is counteracted by the relaxation of system (I) which tends to approach the temperature T_0 of the heat bath.

absorption (or emission, lower sign) is at frequency ν_I, while the system (S) remains at the temperature T_0 of the heat bath with resonance absorption at frequency ν_S.

Therefore, in the limit of validity of (21), we can make the following approximations in order to linearize eqs. (18):

$$\frac{P}{P_0} \simeq 1 , \qquad 1 - P_0 P \simeq 1 - P^2 \equiv 1 - P_0^2 .$$

On the other hand, from (16) and (19), keeping in mind the above approximation, we have at the stationary state

$$\mu_3 - \mu_1 = \frac{2\pi\hbar(\nu_S \pm \nu_I)}{1 + (T_I/T_{S^*})\big((P - P_0)/(P - p_0)\big)} \to 0 ,$$

$$\mu_2 - \mu_1 = \frac{\pm 2\pi\hbar(\nu_S \pm \nu_I)}{1 + (T_{S^*}/T_I)\big((P - p_0)/(P - P_0)\big)} \to \pm 2\pi\hbar(\nu_S \pm \nu_I) ,$$

which, if $w_I = 0$, are satisfied when

$$\frac{T_{S^*}}{T_I} = \frac{(N/n)\beta(1 - P_0^2)}{\alpha/(1 + \alpha\sigma) + \beta/(1 + \beta\sigma)} \to 0 . \tag{22}$$

The linearization and consequently the limit case $p \to \pm P$, are verified when the ratio (22) vanishes.

In the case $\sigma \ll 1$, then $T_{S^*}/T_I = (N/n)\beta(1 - P_0^2)$, which implies high magnetic fields and low temperatures. On the contrary, in the case $\sigma \gg 1$, then $T_{S^*}/T_I = (N/n)\beta(\sigma + 1)(1 - P_0^2)$ (since $\alpha \simeq 1$, $\beta \ll 1$) and (22) is no longer satisfied for high fields and low temperatures; in this case $\sigma \propto H_0^4/T$ and $\sigma \propto H_0^2/T$ for Kramers and non-Kramers doublets respectively.

In any case the presence of a marked phonon bottleneck ($\sigma \gg 1$) strongly limits the possibility of reaching high polarizations, and also affects the linearization of eq. (18).

Anticipating some experimental results we can show that the behaviour and the absolute value of the relaxation times ratio, in the range of temperatures where the direct relaxation process prevails over other types of processes, is in agreement with the theory.

In our case, for the crystals of $La_2Mg_3(NO_3)_{12} \cdot 24H_2O$ doped with 1% and 3.5% of neodymium, the experimental values of relaxation times show the prevailing presence of an Orbach process above 3 °K.

In Fig. 3 the ratios of the experimental relaxation times are shown as a function of temperature for a field of 6370 G. One can note, that the values

for the 1% crystal satisfies the limit condition (22) better than the 3.5% crystal values. Thus we expect better agreement with theoretical predictions deriving from the linearization of (18) for the former crystal. The curves represent the best fit of the experimental values obtained by using the formula

$$\frac{T_{S^*}}{T_I} = \beta' \left(a \operatorname{tgh} \frac{2\pi\hbar\nu_S}{2kT_0} + 1 \right) \operatorname{sech}^2 \frac{2\pi\hbar\nu_S}{2kT_0},$$

where the presence of phonon bottleneck, in the direct process, is evidenced by

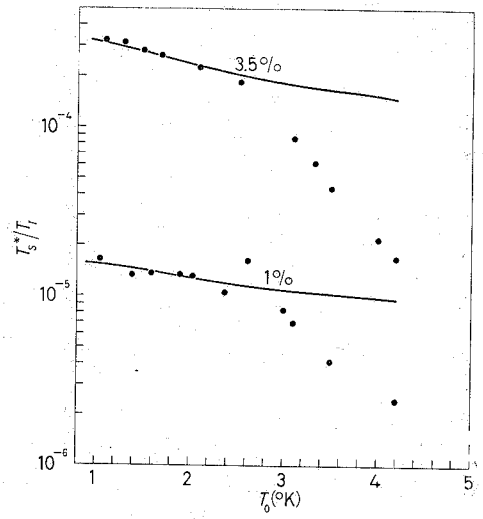

Fig. 3. – T_{S^*}/T_I *vs.* temperatures for two ion concentrations showing reasonable agreement with the function $(N/n)\beta(\sigma+1)(1-P_0^2)$ below $\simeq 3$ °K.

$$\sigma = \tau \frac{w}{P_0} \frac{\frac{1}{2} N 2\pi\hbar\nu_S P_0}{\frac{1}{2} \Delta Q 2\pi\hbar\nu_S P_0^{-1}} \equiv a P_0 .$$

We find the following values for the constants appearing in the above relationship:

$$\left.\begin{aligned} a &\simeq 5 \\ \beta' &\simeq 6 \cdot 10^{-6} \end{aligned}\right\} 1\% ,$$

$$\left.\begin{aligned} a &\simeq 15 \\ \beta' &\simeq 5 \cdot 10^{-5} \end{aligned}\right\} 3.5\% .$$

The value of a for 1% crystal is consistent with the value calculated from ion-lattice relaxation time ($a_{\text{calc}} \simeq 4$). On the contrary for the 3.5% crystal there is disagreement.

From β' we can deduce β: $\beta_{\text{exp}} \simeq 7 \cdot 10^{-2}$ and $\beta_{\text{exp}} \simeq 24 \cdot 10^{-2}$ for the two crystals respectively. The value of this parameter calculated in Appendix B by using a particular model is $\beta_{\text{calc}} \simeq 9 \cdot 10^{-3}$. Hence these results appear inconsistent. But if one takes into account the real structure of the crystals, one has the calculated ([25]) value, $\beta_{\text{calc}} \simeq 6 \cdot 10^{-2}$, which is close to the experimental value for the 1% crystal. As matter of fact there is also agreement with the case of the 3.5% crystal, if one keeps in mind that the dependence of proton relaxation time is not linear in N^{-1}. Approximately, there is an N^{-3} law for high concentration ([26]). Then one obtains $\beta_{\text{exp}} \simeq 4 \cdot 10^{-2}$.

([25]) M. BORGHINI: *Phys. Rev. Lett.*, **16**, 318 (1966).

([26]) G. M. VAN DEN HEUVEL, C. T. C. HEYNING, T. J. B. SWANENBURG and N. J. POULIS: *Phys. Lett.*, **27 A**, 38 (1968).

When the condition (22) is verified and the width of the ion line at frequency ν_s is much smaller than the frequency ν_I, the coupled equations (18) give a solution for one of the two quantities W_+ and W_-.

Indeed, in this case, the frequency of the pumping radiation is one of the two side frequencies, and one has

$$(23) \qquad \begin{cases} p = \dfrac{p_0(1 + T_{s^*}\beta W) \mp T_I(N/n)\beta W P_0}{1 + (1 + f^*)T_I(N/n)\beta W}, \\ P = \dfrac{P_0 \mp T_{s^*}\beta W p}{1 + T_{s^*}\beta W}, \end{cases}$$

where

$$f^* = \frac{n}{N}\frac{T_{s^*}}{T_I} = \frac{n}{N}\frac{T_s}{T_I}(\sigma + 1) \qquad \text{and} \qquad T_{s^*} = T_s(\sigma + 1)$$

is the measured spin heat-bath relaxation time. The upper sign is for the transition at frequency ν_- and the lower one for ν_+.

5. – Experimental apparatus.

The experimental apparatus consists of two spectrometers (Fig. 4), one operating in the microwave frequency band and the other one in the radio frequency band. The essential microwave apparatus part is a TE_{011} tunable

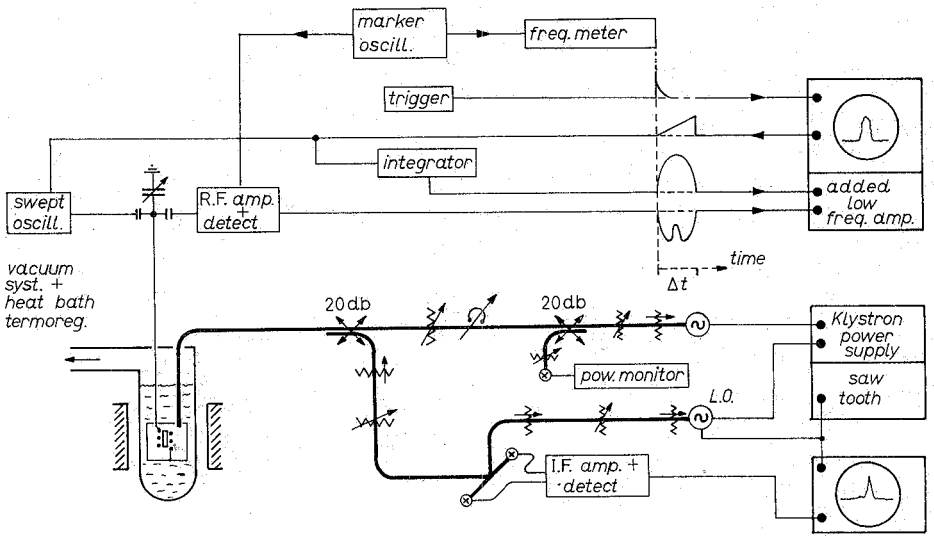

Fig. 4. – Block diagram of the experimental apparatus.

silvered cavity at $\nu_S \simeq 24\,000$ MHz; it is fed by an OKI-24V11 frequency generator of $\simeq 800$ mW nominal power. The cavity containing the sample is immersed in a liquid helium bath whose temperature is thermoregulated within $\simeq 10^{-3}$ °K, in the range from 4.2 °K to about 0.95 °K, by using a standard pump system (nominal pumping speed $\simeq 1000$ l/s) and standard electronic device.

The conventional helium and nitrogen glass dewars, are placed between pole pieces of a magnet with a relative field homogeneity $\sim 10^{-4}$ or better within a $\sim (7 \times 1^2 \pi)$ cm^3 volume, and a field fluctuation $\leqslant 10^{-5}$ G.

The cavity is coupled to the feeding wave guide through a continuously tunable iris, which allows for changes of the reflection coefficient, Fig. 5. The reflected power at frequency ν_S from the cavity is controlled continuously by transferring it into a signal at an intermediate frequency, $f_{IF} = 30$ MHz. This is accomplished by using a linearly swept local oscillator in order to have a frequency mixing, $\nu_S - f_{I0} = 30$ MHz.

At the same time the proton signal is observed as an absorption (or emission) on the response of an oscillating LC circuit tuned at the frequency $\nu_I \simeq 27$ MHz.

The sample is wound by a coil inside the cavity; it is glued, by means a silicon grease drop, on a small teflon pedestal fixed to the cavity top.

The radio frequency oscillator is linearly frequency-swept, in a range $\Delta\nu_I \simeq 5$ times the line width of the proton resonance, by using a saw-tooth modulation (through a varactor).

The saw-tooth modulation has a duration of Δt seconds and is repeated every t seconds.

A typical duty cycle is $\Delta t/t = 10^{-3}$ with Δt equal to a few milliseconds. The response signal, approximatively of parabolic shape, represents the top of the voltage at the LC tuned oscillating circuit. An inverted parabolic signal shape, formed with the same saw-tooth, is summed to this signal. Thus on an oscillograph screen one has an approximatively rectilinear base line syncronized with the saw-tooth.

Upon this base line the proton resonance signal is superimposed.

The saw-tooth duration and its repetition time are varied so that the average power, dissipated in the sample, is reduced by the ratio $\Delta t/t$ with respect to the one of the case of a continuous wave. This device, which is a simplified version of a more complicated ([27]) one, permits us to use oscillator power levels sufficiently high for having good sensibility and rapidity in the measurements. Moreover, it does not saturate the enhanced proton signal when the relaxation times are very long.

([27]) M. BORGHINI, P. ROUBEAU and C. RYTER: *Nucl. Instr. Meth.*, **49**, 248 (1967).

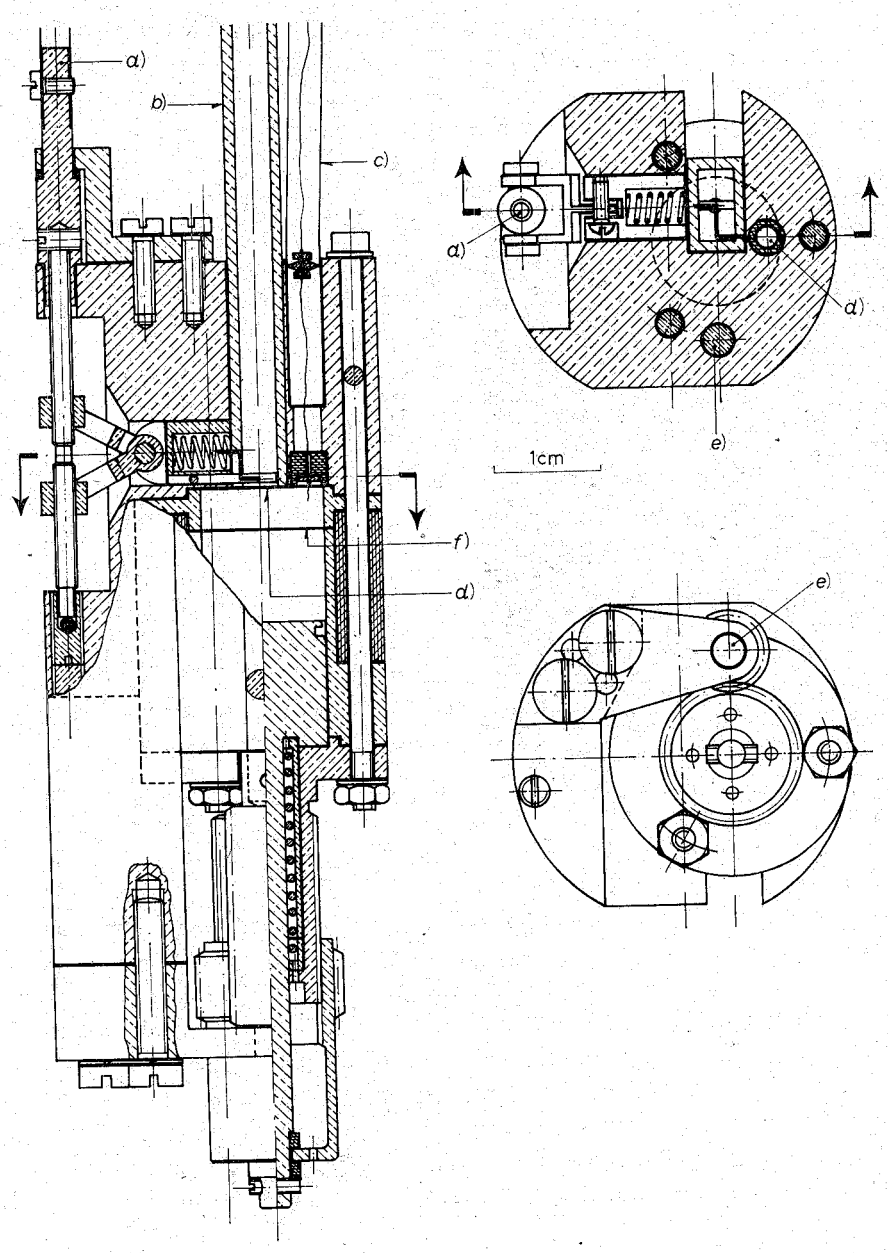

Fig. 5. – Drawing of the TE_{011} cavity: *a*) rod to move stub on iris coupling between cavity and guide; *b*) copper wave guide about 15 cm long. A stainless steel guide (not shown) (0.03 cm thickness), one meter long, is soldered to the closing dewar flange, separated from the microwave apparatus with 1 mill sheet mylar; *c*) coaxial cable made by a stainless steel tube (0.01 cm, thickness), with teflon spacers; *d*) cavity top made with a silvered phosphor bronze sheet (0.03 cm thickness); *e*) rod to move the cavity piston; *f*) the cavity is made by two parts divided with a mylar sheet ring (1 mm thickness).

The photo of Fig. 6 shows an example of a decaying proton signal detected by the repetitive method. In any case the sensibility of this method is by far less than that of the syncronous narrow-band detection method, which has also been used to detect the proton signal, S_0, in thermal equilibrium with the heat bath.

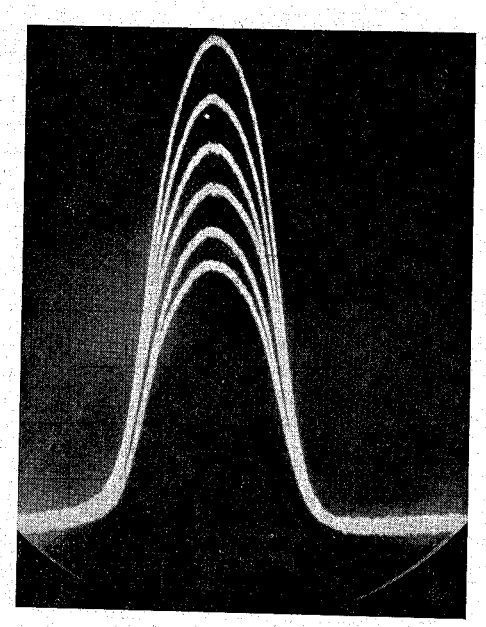

Fig. 6. – Example of decaying proton signal, trace about 300 kHz, photos switched on every 20 s.

In our case, as the sample was small ($\simeq (5\times3\times2)\,\mathrm{mm}^3$), the proton signal could not easily have been detected by the former method. The use of the latter method implies very low level of the radiofrequency power (H_1 in the coil $< 10^{-4}$ G) in order to not saturate the proton signal. This second method has been used to calibrate the proton signal on the oscillograph screen amplified a few times by dynamic pumping.

The polarization values we quote have been obtained by measuring the signal ratio, S/S_0, of the enhanced signal to the thermal equilibrium signal and by using the relation

$$p = p_0 \frac{S}{S_0}\left(1 \pm \left|\frac{\Delta V}{V_0}\right|\right),$$

where $|\Delta V/V_0|$ is the maximum percentage variation of voltage of the radio frequency circuit at the proton resonance, V_0 is the resonance voltage of the oscillating circuit, and the upper and lower signs correspond to the case $p < 0$ and $p > 0$ respectively. The correction $\Delta V/V_0$ is due to the inevitable lack of linearity of the Q-meter to high values of polarization ([27]).

An approximated value of microwave power needed to achieve half of the maximum polarization can be obtained by using relation (23) or (24). The mean squared microwave magnetic field $\langle H_1^2\rangle_{sa}$ on the sample inducing transitions at the frequency $\nu_+ = \nu_S + \nu_I$ can be obtained from the relation

$$\langle H_1^2\rangle_{sa} \doteq \frac{2\,\Delta H_{\frac{1}{2}}}{\gamma_S (N/n)\beta T_I (1+f^*)} \quad (\mathrm{G}^2)$$

where $\Delta H_{\frac{1}{2}}$ is the half-width at half intensity of the ion absorption line.

From the definition of Q_L loaded cavity factor, $Q_L = 2\pi\nu_S E/P_i(1-\Gamma^2)$, where E (J) is the stored energy, P_i (W) is the incident power on the cavity,

Γ^2 is the power reflection coefficient, one has:

$$P_i = \frac{10^{-7}}{4Q_L(1-\Gamma^2)} \nu_S V_{ca} [1.35 \cdot 10^{-1} \langle H_1^2 \rangle_{sa}] \text{ W},$$

where V_{ca} (cm^3) is the cavity volume, ν_S in Hz and

$$1.35 \cdot 10^{-1} \langle H_1^2 \rangle_{sa} \simeq \langle H_1^2 \rangle_{ca} \text{ (*)}.$$

Since we have $V_{ca} \simeq 3$ cm^3, $Q_L \simeq 2000$, $\Gamma^2 \simeq 0$, for the crystal 1% neodynium doped one has $P_i \simeq 7$ μW at 2 °K and $P_i \simeq 3$ mW at 4.2 °K.

The power thus calculated is that dissipated in the cavity (walls, r.f. coil, dielectric losses in the sample, imperfections). The power absorbed by the sample in order to build up the proton polarization, is given by

$$P_{sa} \simeq W_+ 2\pi\hbar\nu_S N P_0 V_{sa} = \frac{2\pi\hbar\nu_S P_0 V_{sa} n}{T_1(1+f^*)} \text{ W}$$

for a well resolved line.

It gives $P_{sa} \simeq 2\mu$ W at 2 °K and $P_{sa} \simeq 1$ mW at 4.2 °K. These values are about a factor 3 less than the power dissipated for cavity losses.

For a 3.5% doped crystal the total power increases by about a factor of ten.

6. – Measurements and interpretation.

The dynamic polarization and the spin relaxation times of protons in the hydration water of $La_2Mg_3(NO_3)_{12} \cdot 24H_2O$ (**) single crystals doped with 1% and 3.5% of neodymium, have been measured in a magnetic field $H_0 = 6370$ G, in the temperature range from 4.2 °K to 1 °K.

The measurements have been performed at an angle $\theta \geqslant 85°$ between the direction of the magnetic field and the optical axis of the crystals.

The dynamic polarization as a function of the pumping power at frequency $\nu_+ = \nu_S + \nu_I$ for various temperatures are shown in Fig. 7 and 8; similar results, but with opposite sign, have been found at frequency $\nu_- = \nu_S - \nu_I$.

(*) This relation is valid in the case when the electromagnetic field distribution in the cavity is not altered. In our case this is not strictly true, since in the space region of maximum field a coil and a sample are placed. Consequently the real values of powers are greater than that calculated.

(**) The single crystals are grown from a saturated solution of magnesium nitrate (analytical Mallinckrodt), lanthanum nitrate (purity 99.997) and neodymium nitrate (99.9, both from American Potash and Chemical Corporation) in the right stoichiometric ratio in a temperature bath at 0 °C.

From these measurements it is possible to deduce the maximum polarization for the highest limit values of the power by extrapolating the data ob-

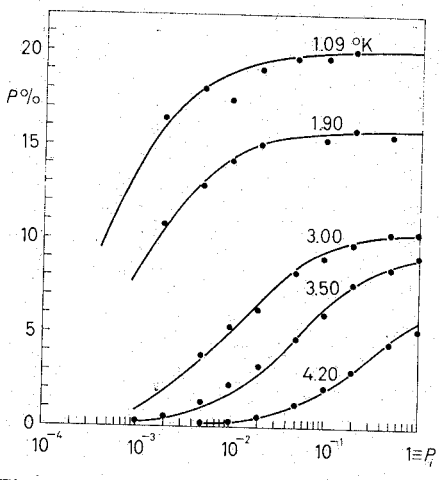

Fig. 7. – Proton dynamic polarization *vs.* microwave power, for crystal doped with 1% of neodymium, $P_i \simeq 60$ mW.

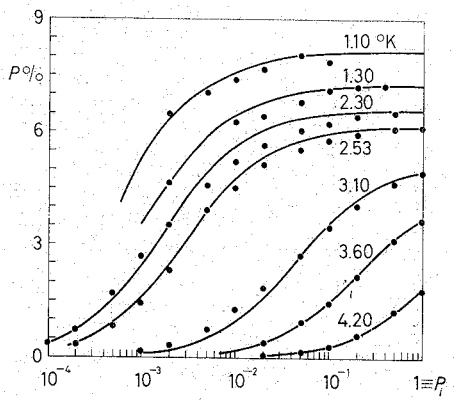

Fig. 8. – The same as in Fig. 7, but for the crystal doped with 3.5% of neodimium.

tained where the saturation process is not yet in evidence (Fig. 9 and 10); moreover the relative values of the power for half maximum polarization are deduced (Fig. 11). These data must be compared with the results of the theory.

If we disregard the term

$$p_0(1 + T_{s^*}\beta W) \ll T_1(N/n)\beta W P_0 ,$$

the proton polarization expression (23) is rewritten in the form

$$(24) \qquad p = \frac{P_0}{1 + f^*} \frac{W(\nu)}{W_{\frac{1}{2}} + W(\nu)} ,$$

where

$$W_{\frac{1}{2}} = \left[\frac{N}{n}\beta T_1(1 + f^*)\right]^{-1} ,$$

$$W(\nu) = \frac{1}{4}\gamma_S^2 H_1^2 g(\nu) ,$$

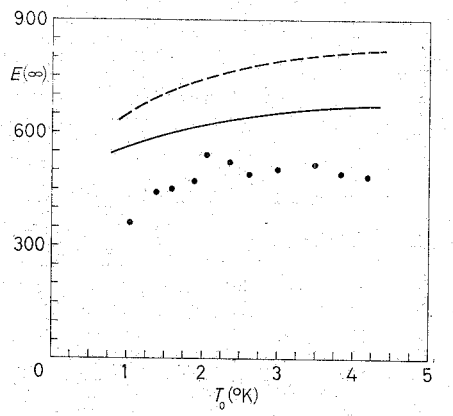

Fig. 9. – Maximum value of proton enhancement *vs.* temperature for crystal doped with 1% of neodymium; dashed line is for solid effect, while the continuous one is for the direct cooling theory.

and $g(\nu)$ is the absorption-line shape, such that

$$\int_0^\infty g(\nu)\,\mathrm{d}\nu = 1\,,$$

with central frequency ν_s and with the maximum value $g(\nu_s) = 2(\gamma_s \Delta H_{\frac{1}{2}})^{-1}$.

From (24) the expressions $p(\infty) = P_0(1 + f^*)^{-1}$ and $W_{\frac{1}{2}}$ are determined when the parameter $f^* = (n/N)(T_{s^*}/T_1)$ is determined, that is when the para-

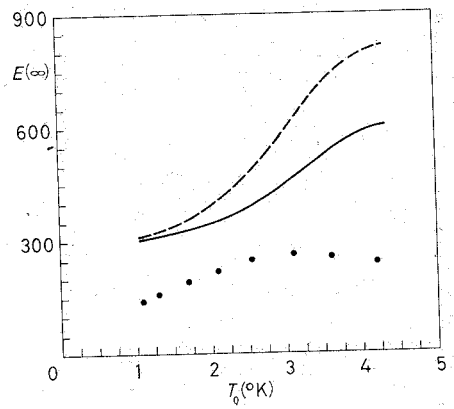

Fig. 10. – The same as in Fig. 9, but for crystal doped with 3.5% of neodymium.

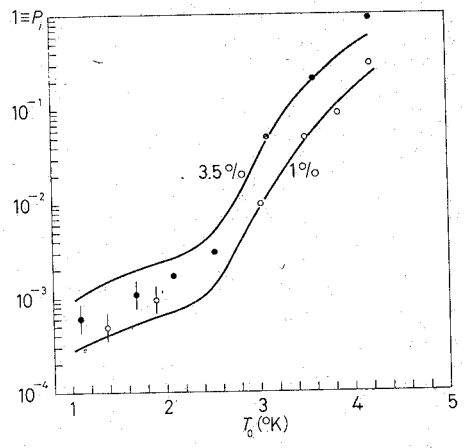

Fig. 11. – Microwave power for half of the maximum polarization *vs.* temperature.

magnetic ion concentration and the relaxation times are known. It has been found that the crystals, growing in a saturated solution of LaMN with Nd^{3+}, contain an ion concentration about five times less than in the solution [27-29].

From paramagnetic measurements, by using a conventional spectrometer at $\simeq 24$ GHz, the ratio of ion concentrations in the two crystals is determined: we found the value 2.5 instead of 3.5 as in solution.

Since the site numbers of lanthanum in a cubic centimeter are known, one deduces in a simple way the N value for each crystal.

The proton relaxation times have been measured, in the two crystals (Fig. 12) while the ionic one is deduced by using expression experimentally verified by other authors [30,4]. Since no measurements have been made up

---

[28] G. SHAPIRO: private communication.
[29] T. J. B. SWANENBURG: *Physica*, **35**, 369 (1967).
[30] J. M. BAKER and N. C. FORD: *Phys. Rev.*, **136**, A 1692 (1964).

to now at 6370 G, we extrapolate and average data above and below this field (Fig. 12) by computing the expression

$$T_{s^*}^{-1} = 6 \cdot 10^9 \exp\left[-\frac{47}{T_0}\right] + \left\{\left[50\left(\frac{h\nu_S}{2k}\right)\mathrm{ctgh}\left(\frac{h\nu_S}{2kT_0}\right)\right]^{-1} + \right.$$
$$\left. + \left[23\left(\frac{h\nu_S}{2k}\right)^2 \mathrm{ctgh}^2\left(\frac{h\nu_S}{2kT_0}\right)\right]^{-1}\right\}^{-1} \mathrm{s}^{-1}.$$

This expression was used for both crystals with 1% and 3.5% of neodymium, since the existing experimental data show ([31-33]) a low dependence of T_{s^*} on concentration of the paramagnetic ions in LaMN, as already noted. Therefore we can assume the same relaxation time for our crystals.

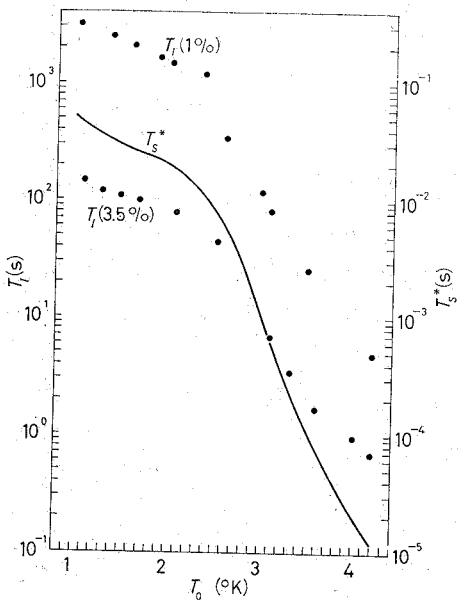

Fig. 12. – Experimental proton relaxation times T_1 for the two crystals, and ion relaxation time deduced from other authors.

In Table I we report the numerical values of the relaxation times, of the f^* factor, of the $E(\infty) = p(\infty)/p_0$ maximum enhancement, and of the quantity $C^{-1}(n/N)[T_1(1 + f^*)]^{-1}$, where the constant C is determined by equating the theoretical and experimental values at 3.6 °K for the crystal at 3.5%.

The expression (24) gives the proton polarization as a function of $W \propto H_1^2$, a quantity proportional to the microwave power. Its behaviour is shown by continuous lines in Fig. 7 and 8 and there is a fairly good agreement with the experimental values, with the exception of some discrepancies for the 3.5% crystal. In Fig. 11 the relative values of incident power on the cavity for which half-polarization sets up as a function of temperature are shown. The experimental points on the vertical line are extrapolated to low power from curves of Fig. 6 and 7, while the curves represent the function $[C(N/n)\,T_1(1 + f^*)]^{-1}$ for the two crystals.

([31]) R. H. RUBY, N. BENOIT and C. B. JEFFRIES: *Phys. Rev.*, **127**, 51 (1962).
([32]) J. RAMAKRISHNA: *Indian Journ. Pure Appl. Phys.*, **5**, 565 (1966).
([33]) E. J. VERWEY: *Phys. Lett.*, **28 A**, 152 (1968).

TABLE I. – *The relaxation times T_I, T_{S^*}, the leakage factor f^*, the relative power for half maximum polarization and the maximum enhancement* (24).

Crystal	n/N	T (°K)	T_{S^*} (ms)	T_I (s)	f^*	$C^{-1}(n/N)\cdot[T_{In}(1+f)]^{-1}\cdot 10^4$	$E_{th}(\infty)$
1 %	$12\cdot10^3$	4.20	0.012	4.9	0.030	2200	850
		3.50	0.11	26	0.050	400	830
		3.10	0.59	82	0.086	125	800
		3.00	0.99	120	0.100	84	790
		2.62	5.7	350	0.19	27	730
		2.38	12.8	1200	0.13	8.2	760
		2.03	19.8	1500	0.16	6.3	730
		1.90	22.1	1650	0.16	5.7	730
		1.39	31.1	2500	0.16	3.8	710
		1.04	52.5	3200	0.20	2.9	660
3.5%	$4.8\cdot10^3$	4.20	0.012	0.69	0.084	6000	810
		4.00	0.021	0.95	0.104	4250	800
		3.59	0.080	1.7	0.226	2100	715
		3.32	0.222	3.5	0.305	970	665
		3.10	0.59	6.9	0.41	450	620
		2.53	8.4	45	0.90	54	450
		2.09	18.7	83	1.08	26	410
		1.49	31.0	110	1.35	17.5	350
		1.30	37.9	120	1.51	14.8	320
		1.10	48.3	149	1.56	11	310

The relative power measurements are effected by systematic and casual errors of few decibels; this fact is essentially due to the lack of constancy in the power coupling of the system wave-guide–cavity, when temperature is varied, and to different sample coil geometries for the two crystals.

Owing to this fact one notes satisfactory agreement between theoretical behaviour and experimental points. Moreover, since the incident power on the cavity is estimated to be about 60 mW, (that is P_i in Fig. 7-11 is equivalent to that value), one notes also a fairly good agreement of the absolute values (see the preceding paragraph).

The experimental values of $E(\infty) = p(\infty)/p_0$ are shown in Fig. 8 and 9, where also the behaviour of (24) (dashed line) is represented. One notes a strong discrepancy between experimental points and calculated values, especially for the crystal at 3.5%.

The maximum polarization is reduced by the effects already discussed, that is the phonon bottleneck effect ($\sigma > 1$), and the leakage effect ($f^* \neq 0$) ([29,34]),

([34]) T. J. B. SWANENBURG, R. BOOY and N. J. POULIS: *Physica*, **37**, 65 (1967).

and also by other effects such as impurities ($w_I \neq 0$), interaction among ionic spins, effects due to cross relaxations between spin packets of different resonance frequency, and mainly by the effect due to the finite line widths of ionic spectrum.

The hypothesis that the line width, $\simeq 2\nu_L$, of the ionic resonance at frequency ν_S is very narrow, that is $\nu_L \ll \nu_I$, is verified only in the ideal case which is known as the pure solid effect. Only in this last case the maximum enhancement is always at the pumping frequency $\nu_S \pm \nu_I$. This fact was experimentally verified for fields of the order of or greater than 10 kG ([4]); on the contrary we find the maximum enhancement at a frequency smaller than ν_+ or greater than ν_-, for increasing powers.

This effect is deduced from the more general theory ([35]), which takes account of the finite line width at frequency $\nu_S \pm \nu_I$ and ν_S. On the other hand direct measurements of line widths give $2\nu_L \simeq 23$ MHz (about 6 G) for the crystal at 1%, and $2\nu_L \simeq 25$ MHz ($\simeq 6.6$ G) for the crystal at 3.5%. Therefore we are far from the condition $\nu_L \ll \nu_I$, since $\nu_I \simeq 27$ MHz.

The exact formulation of the dynamic polarization problem with the formalism of density matrix ([8,9]) is mathematically difficult.

These difficulties are overcome only in the « high-temperature approximation », that is when the condition $h\nu_S/2kT_0 \ll 1$ is verified. As our experimental conditions are $0.15 \leqslant h\nu_S/2kT_0 \leqslant 0.6$ for $1\ ^\circ\mathrm{K} \leqslant T_0 \leqslant 4.2\ ^\circ\mathrm{K}$ then we are near the limit condition to use the results of such approximation. However for the maximum enhancement this theory gives the expression

$$E(\infty) = \frac{p(\infty)}{p_0} = \frac{\nu_S}{2\sqrt{2\nu_L^2 + f^* \nu_I^2}}.$$

Its behaviour is plotted in Fig. 9 and 10 (continuous line), and one notes better agreement with the experimental points.

This fact shows the presence of a direct cooling, as predicted by the general theory and already found at lower magnetic fields ([29,34]). However the discrepancy, for the 3.5% crystal, is still too strong. Probably the extrapolated values of polarizations above 3 °K are smaller than the real ones, because the available maximum power is not sufficient to reach the state of saturation (see Fig. 8). Moreover a certain number of satellite lines are observed on both sides of frequency ν_S spread over some hundred gauss, with total area of $\simeq 8\%$ with respect to the central one, for 3.5% crystal. Such lines were not observed in the crystal having 1% Nd impurities.

([35]) A. ABRAGAM and M. BORGHINI: *Progr. Low Temp. Physics*, vol. 4 (Amsterdam, 1964), p. 384.

The presence of such lines gives rise to cross-relaxation effects which influence the relaxation times and the dynamic polarization.

We must now recall the approximation made about the use of the same ion spin-bath relaxation time for the two crystals. Indeed this single value for T_{s^*} has been used in order to perform a comparison with the theory. Thus, at least partially, the observed discrepancies in the 3.5% crystal may be caused by this approximation.

Concluding this work we may state that, except for some disagreements understandable by using convenient mechanisms ([4,29,34,36-38]), the experimental results are in good agreement with the present theories on dynamic polarization.

Better agreement with formula (24) should be obtained in measurements at higher magnetic field. In fact, as the resonance line broadening is not much affected by the magnetic field, the condition $\nu_L \ll \nu_I$ should be well verified.

APPENDIX A

We shall calculate the dipolar interaction effects on the allowed and forbidden paramagnetic transitions at frequencies $\nu_S, \nu_\pm$ respectively. First we shall consider a system of one electron spin and n nuclear spins (protons) immersed in an external magnetic field H_0. The Hamiltonian of such a system is

$$\mathcal{H} = |\gamma_S| \hbar \bar{H}_0 \cdot \bar{S} - \gamma_I \hbar \bar{H}_0 \sum_{j=1}^{n} \bar{I}_j + \sum_{j=1}^{n} \mathcal{H}_{\text{dip}}(j) \,, \tag{A.1}$$

where $\mathcal{H}_{\text{dip}}(j)$ is the dipolar interaction between the electron spin and the j-th nuclear spin and $|\bar{S}| = |\bar{I}| = \frac{1}{2}$. If the dipolar interaction is small compared with the Zeeman energies, the energy levels of (A.1) are those shown in Fig. 13 ([39]).

There are $n+1$ nuclear levels for every possible electron spin orientation. These levels are degenerate, because the same energy pattern is obtainable by changing the nuclear spins. So, *e.g.*, the level 1, corresponding to the case when the electron spin and one nuclear spin are both opposite to the field and the other nuclear spins are along the field direction, can be obtained in n ways, because it is possible to choose the nuclear spin with « spin down » between n nuclear spins. We label the n degenerate states of the level 1 by the index l. The level 2 corresponds to the case of the electron spin and two nuclear spins

---

([36]) T. J. B. SWANENBURG, G. M. VAN DEN HEUVEL and N. J. POULIS: *Physica*, **33**, 707 (1964).

([37]) M. BORGHINI: *Phys. Lett.*, **26** A, 242 (1968).

([38]) M. BORGHINI: *Phys. Lett.*, **20**, 228 (1966).

([39]) J. H. VAN VLECK: *Phys. Rev.*, **74**, 1168 (1948).

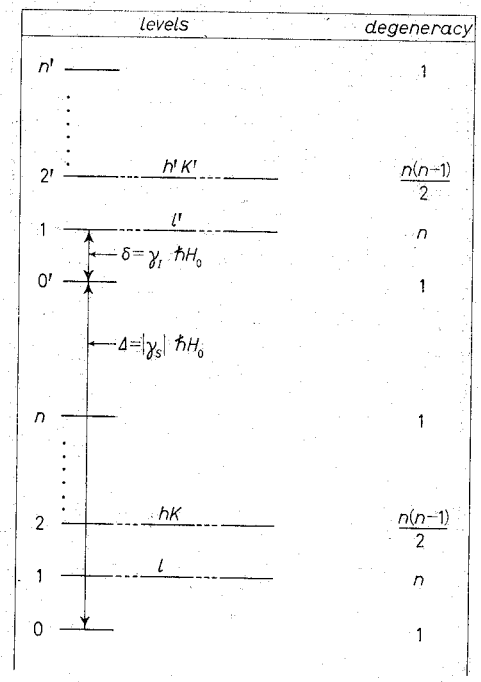

Fig. 13. – Pattern of energy levels for one electron spin and n proton spins in dipolar coupling.

« down ». There are $n(n-1)/2$ ways to choose the two nuclear spins and the corresponding states are labelled by the indexes $h<k$, and thus for the other levels. The same procedure is repeated for the levels $0', 1', \ldots, n'$ in which the electron spin is directed along the field direction.

Actually the dipolar interaction between the nuclear spins resolves the above degeneration, but its effect is practically negligible because the nuclear-nuclear interaction is smaller than the electron-nuclear one.

The effects of the dipolar static interaction $\sum_j^n \mathscr{H}_{\text{dip}}(j)$ are both a shift of the energy levels, which we disregard, and a mixing between close states. The dipolar interaction matrix elements calculated between the states are responsible for their mixing. Without entering into the question, already known in the literature [14], we give some general results.

The state 0 is mixed with all the states of the level 1. The state l of the level 1 is mixed with 0 and with $n-1$ states of the level 2 for which $h=l$; the matrix elements between states for which $h \neq l$ vanish. At last the wave functions of the new perturbed states are:

$$\text{(A.2)} \qquad \begin{cases} \psi(0) = A\Big[\psi_0(0) - \sum_l^n \varepsilon_l \psi_0(l)\Big], \\ \psi(l) = A\Big[\psi_0(l) + \varepsilon_l^* \psi_0(0) - \sum_{k\neq l}^n \varepsilon_k \psi_0(l,k)\Big], \\ \vdots \\ \psi'(0') = A\Big[\psi_0'(0') + \sum_{l'}^n \varepsilon_{l'} \psi_0'(l')\Big], \\ \psi'(l') = A\Big[\psi_0'(l') - \varepsilon_{l'}^* \psi_0'(0') + \sum_{k'\neq l'}^n \varepsilon_{k'} \psi_0'(l',k')\Big]. \end{cases}$$

$\psi_0(0)$, $\psi_0(l)$, $\psi_0(h,k)$, ..., $\psi_0'(0')$, $\psi_0'(l')$, $\psi_0'(h',k')$, ... are the wave functions of the unperturbed states, $A = \Big(1 + \sum_j \varepsilon_j^2\Big)^{-\frac{1}{2}}$ a normalization factor, and ε reads

$$\text{(A.3)} \qquad \varepsilon_j = \frac{\langle m+1|\mathscr{H}_{\text{dip}}(j)|m\rangle}{E(m+1)-E(m)} = \frac{3}{4}\frac{\gamma_S \hbar}{R_j^3 H_0} \sin\theta_j \cos\theta_j \exp[i\varphi_j].$$

R_j, θ_j and φ_j are the polar co-ordinates of the nuclear spin j with respect to a system centred on the electron spin and with the z-axis directed parallel to the magnetic field.

A time-dependent perturbation $\mathscr{H}(t)$ induces transitions between the levels. The probabilities of such transitions are proportional to the matrix elements of $\mathscr{H}(t)$ calculated between the level states. We write for the unperturbed system

$$\text{(A.4)} \qquad \begin{cases} \langle \psi_0(0)|\mathscr{H}(t)|\psi_0'(0')\rangle = V_s\,, \\ \langle \psi_0(l)|\mathscr{H}(t)|\psi_0'(l')\rangle = V_s\delta_{ll'}\,, \\ \langle \psi_0(h,k)|\mathscr{H}(t)|\psi_0'(h',k')\rangle = V_s\delta_{hh'}\,\delta_{kk'}\,, \end{cases}$$

while the matrix elements such as $\langle 0|\mathscr{H}(t)|1'\rangle$, $\langle 0|\mathscr{H}(t)|2'\rangle$, $\langle 1|\mathscr{H}(t)|0'\rangle$ etc. are identically zero. If $\mathscr{H}(t)$ is the perturbation which includes the relaxation process, then $T_{s^*}^{-1} \propto |V_s|^2$. Hence it is possible, by bearing in mind the relations (A.4), to calculate the matrix elements of $\mathscr{H}(t)$ between the perturbed states (A.2). For the transition 0-0′ the result is

$$\text{(A.5)} \qquad \langle \psi(0)|\mathscr{H}(t)|\psi'(0')\rangle = A^2\Big(1-\sum_j^n \varepsilon_j^2\Big)\,V_s\,;$$

the transitions 1-1′, 2-2′ etc. give identical results. For the electron-nuclear (0-l') transition, we have

$$\text{(A.6)} \qquad \langle \psi(0)|\mathscr{H}(t)|\psi'(l')\rangle = -2A^2\varepsilon_{l'}^*\,V_s$$

and so on for the other formerly forbidden transitions, with a difference of the sign or with ε_l in the place of its complex conjugate ε_l^*.

We are now able to calculate the transition probabilities between the perturbed levels. From (A.5) and by putting $W_s \propto |V_s|^2$, the electron transition probability $W(\Delta)$ reads

$$\text{(A.7)} \qquad W(\Delta) = \frac{\Big(1-\sum_j^n \varepsilon_j^2\Big)^2}{\Big(1+\sum_j^n \varepsilon_j^2\Big)^2}\,W_s\,.$$

The electron–j-th proton transition probability $W(\Delta \pm \delta)_j$, from (A.6), is

$$\text{(A.8)} \qquad W(\Delta \pm \delta)_j = \frac{4\varepsilon_j^2}{\Big(1+\sum_j^n \varepsilon_j^2\Big)^2}\,W_s\,.$$

These results are valid in a system of one electron and n nuclear spins (protons). We can extend them to a system of N electrons $(1, 2, \ldots, i, \ldots, N)$

and n protons, assuming a negligible dipolar interaction between N paramagnetic ions (that is in the case when the ion concentration is very small), and $N \ll n$.

It is evident from (A.8) that the probability for a proton flip is strongly dependent on its distance from the electron spin, $W(\Delta \pm \delta) \propto R_j^{-6}$. Hence we can obtain a unique value of the probability for all the protons only in the case of a nuclear spin diffusion faster than the fastest flip between a nuclear spin and an electron spin.

With this hypothesis, enough realistic ([40]), the j-proton flip probability with any electron spin, among the N spins, is simply $\sum_i^N W(\Delta \pm \delta)_{ij}$ and the proton flip probability is the average over all the protons, that is $(1/n) \sum_j^n \sum_i^N W(\Delta \pm \delta)_{ij}$. As the sum $\sum_j \varepsilon_{ij}^2$ does not depend upon i, because of the assumed isotropic distribution of the proton spins around the electron spins, we obtain at last

$$W(\Delta \pm \delta)_{\text{protons}} = \frac{N}{n} \frac{4 \sum_j \varepsilon_j^2}{\left(1 + \sum_j \varepsilon_j^2\right)^2} W_S \,. \tag{A.9}$$

The probability of an electron spin flip with any nuclear spin among the n spins, is obtained by adding the contribution of all nuclear spins in (A.8) and by averaging with respect to the N electron spins. The final result is

$$W(\Delta \pm \delta)_{\text{elect}} = \frac{4 \sum_j \varepsilon_j^2}{\left(1 + \sum_j \varepsilon_j^2\right)^2} W_S \,. \tag{A.10}$$

Hence the probability that an electron spin flips (with a nuclear spin) (A.10) is different from the probability that a nuclear spin flips (with an electron spin) via the dipolar interaction. This difference derives from the particular system we have considered and all these results are valid only when $N \ll n$.

The probability that any electron spin flips by itself is the average of the single probabilities, and is given by the same formula (A.7).

In conclusion, we have for the forbidden transitions, $\nu_\pm = (\Delta \pm \delta)/h$, and the allowed ones, $\nu_S = \Delta/h$, the following expressions:

$$\begin{cases} W(\Delta \pm \delta) = \beta' W_S = \begin{cases} \dfrac{N}{n} \beta W_S & \text{for protons}, \\ \beta W_S & \text{for electrons}, \end{cases} \\ W(\Delta) = \alpha W_S \,, \end{cases} \tag{A.11}$$

([40]) C. D. JEFFRIES: *Proc. Phys. Soc.*, **88**, 257 (1966).

with

$$\alpha = \frac{\left(1 - \sum_j^n \varepsilon_j^2\right)^2}{\left(1 + \sum_j^n \varepsilon_j^2\right)^2}, \qquad \beta = \frac{4 \sum_j^n \varepsilon_j^2}{\left(1 + \sum_j^n \varepsilon_j^2\right)^2}.$$

If $W(\Delta \pm \delta)$ is the general expression for the forbidden transitions probability, its exact expressions depend on whether it refers to nuclear spins or to electron spins.

Appendix B

The factors of the terms $(p - p_0)$ and $(P - P_0)$ in (18) are the inverses of the proton (I) and ion (S) relaxation times respectively. By writing $-w/P_0 = 1/T_s$ they are given by

$$\text{(B.1)} \qquad \begin{cases} T_I^{-1} = T_s^{-1}\beta' \left[\dfrac{1 + \sigma\beta'}{1 + \sigma\beta'(P/P_0)} - P_0 P\right] + 2w_I, \\ T_{s^*}^{-1} = T_s^{-1}\left[\dfrac{1 + \sigma(P/P_0)\left(1 + \alpha\beta\sigma(P/P_0)\right)}{\left(1 + 2\alpha\beta\sigma(P/P_0)\right)}\right]^{-1}, \end{cases}$$

in the limit of the linear approximation and by supposing a nuclear relaxation only via the ionic system S (that is, $w_I = 0$) (B.1) gives

$$\text{(B.2)} \qquad \begin{cases} T_I^{-1} = T_s^{-1} \dfrac{N}{n} \beta(1 - P_0^2), \\ T_{s^*}^{-1} = T_s^{-1}\left[\dfrac{1 + \sigma(1 + \alpha\beta\sigma)}{1 + 2\alpha\beta\sigma}\right]^{-1} \underset{\sigma\beta \ll 1}{\simeq} T_s^{-1}(\sigma + 1)^{-1}. \end{cases}$$

These formulas show the very interesting result that the proton spin-lattice relaxation time is independent of σ in the limit of the linear approximation. Even more it is possible to state that the experimental proton relaxation time, obtained by using the decay method after enhancement, is in any case independent of σ, because $T_I \gg T_s$ and then $P = P_0$ during the proton signal decay. Obviously all these statements are limited by the validity of the model considered until now; see Appendix A.

From (B.2) we note that the relaxation process is strongly influenced by the coefficient β. Its numerical value can be calculated exactly from the crystal structure. Now we obtain an approximated value of this constant from a more simple method. Supposing the protons continuously and isotropically distributed around the paramagnetic ions, we can transform the sum into

an integral, and we have simply

$$\sum_j^n \varepsilon_j^2 = \int_{R_{\min}}^{R_{\max}} \varepsilon_j^2 n \, \mathrm{d}V = \frac{\pi}{10} \left(\frac{\gamma_s \hbar}{H_0}\right)^2 n \left| \frac{1}{R^3} \right|_{R_{\max}}^{R_{\min}} . \tag{B.3}$$

This sum is independent of $R_{\max}$ if $R_{\max} \gg R_{\min}$, where (*) $R_{\min} = R_1$ is the minimum distance between a paramagnetic ion and a nuclear spin. For the LaMN crystals $R_1 = 4.36$ Å, $n = 3.7 \cdot 10^{22}$ protons/cm^3 and $g = 2.7$ ($\theta \simeq 90°$); then $\sum \varepsilon_j^2 \simeq 8.75 \cdot 10^4 / H_0^2$. For magnetic fields higher than 10^3 G, $\beta \simeq 4 \sum \varepsilon_j = 3.5 \cdot 10^5 H_0^{-2}$.

The proton spin-lattice relaxation time by using the value of β from the expression (B.3), becomes

$$T_I^{-1} = T_S^{-1} \frac{4\pi}{10} \left(\frac{\gamma_s \hbar}{H_0}\right)^2 \frac{N}{R_1^3} (1 - P_0^2) . \tag{B.4}$$

This formula is identical with that obtained from the « shell of influence » model [4], if we put $N = (3/4)(1/\pi R_2^3)$ with $2R_2$ equal to the ion average distance. This last position is equivalent to dividing the crystal into spheres with radius R_2. Till now this simple phenomenological model appears the more realistic with respect to the experimental results [4,40,41], at least for small concentrations of para-magnetic ions. Indeed the linear dependence of the inverse of proton spin-lattice relaxation time on the ion concentration is not verified experimentally [26,42,43] for high concentration of Nd^{+3} in LaMN crystals.

(*) Actually $R_{\min}$ in (B.3) does not coincide with R_1, because, the proton-proton distance being generally comparable with R_1 and in this case the protons being distributed two by two, we cannot simply transform the crystal structure into a continuum, especially in the vicinity of a paramagnetic centre where the ε_j^2 gives the major contribute to the sum (B.3).

[41] T. E. GUNTER and C. D. JEFFRIES: *Phys. Rev.*, **159**, 290 (1967).
[42] G. BALDACCHINI and V. MONTELATICI: *Lett. Nuovo Cimento*, **1**, 649 (1969).
[43] J. RAMAKRISNA: *Proc. Phys. Soc.*, **92**, 570 (1967).

RIASSUNTO

La teoria dell'effetto solido è sviluppata da un punto di vista termodinamico e statistico introducendo un potenziale chimico per ciascun gruppo di spin del sistema a seconda del loro stato. La variazione temporale della produzione di entropia è scritta in funzione dei potenziali chimici e delle probabilità di transizione. I meccanismi dei

processi di rilassamento sono specificati, e si considera il bilancio tra l'energia Zeeman, l'energia fononica e il flusso di energia al termostato. In questo modo si ottengono due equazioni accoppiate per la polarizzazione degli ioni e dei protoni, che vengono linearizzate tramite alcune relazioni, tra i potenziali chimici e i tempi di rilassamento, dedotte allo stato stazionario nel caso limite in cui il fattore di Boltzman elettronico è trasferito ai protoni. Il tempo di rilassamento dei protoni e la polarizzazione dinamica a 6370 G nell'intervallo di temperatura dell'elio liquido sono stati misurati in cristalli di LaMN drogato con 1% e 3.5% di ioni neodimio. I valori sperimentali dei tempi di rilassamento sono in buon accordo con la teoria. Discrepanze sono state trovate nella dipendenza del tempo di rilassamento della concentrazione di impurità. I valori sperimentali di polarizzazione dinamica, il cui valore massimo è circa 20%, per il cristallo all'1% mostrano un marcato effetto di raffreddamento diretto via il sistema di elettroni, effetto già osservato a campi più bassi da altri autori.

Вклад в исследование динамической поляризации, обусловленной влиянием твердого тела.

Резюме (*). — Развивается теория влияния твердого тела из термодинамического и статистического подхода, посредством введения химического потенциала для каждой группы спинов системы, согласно их состояниям. Скорость образования энтропии записывается, как функция химических потенциалов и вероятностей переходов. Специализируются механизмы релаксационных процессов и рассматривается энергетический баланс между энергиями Зеемана и фононов и энергетическим потоком к термостату. Таким образом получаются два связанных уравнения для поляризаций ионов и протонов, которые линеаризуются с помощью выведенных соотношений, в стационарном состоянии, между химическими потенциалами и отношением времен ионной и протонной релаксаций, в предельном случае, когда электронный больцмановский фактор передается протонам. Измеряются протонная релаксация и динамическая поляризация при 6370 гаусс, в области гелиевых температур на кристаллах LaMN, с присадкой 1% и 3.5% ионов неодима. Экспериментальные времена релаксации хорошо согласуются с теоретическими значениями. Обнаружены расхождения, касающиеся зависимости времен релаксаций от концентрации примесей. Экспериментальные значения динамической поляризации, максимум которой составляет около 20% для 1% присадки, обнаруживают значительный эффект непосредственного охлаждения за счет электронной системы, эффект, который уже наблюдался при более низких магнитных полях другими авторами.

(*) *Переведено редакцией.*